Impaired Revascularization in a Mouse Model of Type 2 Diabetes Is Associated With Dysregulation of a Complex Angiogenic-Regulatory Network

Stephan Schiekofer, Gennaro Galasso, Kaori Sato, Benjamin J. Kraus, Kenneth Walsh

Objective—Diabetes is a risk factor for the development of cardiovascular diseases associated with impaired angiogenesis or increased endothelial cell apoptosis.

Methods and Results—Here it is shown that angiogenic repair of ischemic hindlimbs was impaired in $Lepr^{db/db}$ mice, a leptin receptor–deficient model of diabetes, compared with wild-type (WT) C57BL/6 mice, as evaluated by laser Doppler flow and capillary density analyses. To identify molecular targets associated with this disease process, hindlimb cDNA expression profiles were created from adductor muscle of $Lepr^{db/db}$ and WT mice before and after hindlimb ischemia using Affymetrix GeneChip Mouse Expression Set microarrays. The expression patterns of numerous angiogenesis-related proteins were altered in $Lepr^{db/db}$ versus WT mice after ischemic injury. These transcripts included neuropilin-1, vascular endothelial growth factor-A, placental growth factor, elastin, and matrix metalloproteinases implicated in blood vessel growth and maintenance of vessel wall integrity.

Conclusion—These data illustrate that impaired ischemia-induced neovascularization in type 2 diabetes is associated with the dysregulation of a complex angiogenesis-regulatory network. (***Arterioscler Thromb Vasc Biol.* 2005;25:1603-1609.)**

Key Words: diabetes ■ ischemia ■ angiogenesis ■ microarrays

Diabetes is associated with microvascular rarefaction and reduced collateralization in ischemic tissues.[1,2] These circulatory deficits often lead to ischemic injury, impaired wound healing, and the development of peripheral artery disease in diabetic patients. The mouse ischemic hindlimb model is used to study angiogenic repair associated with peripheral artery disease.[3] In this model, the distal portion of the saphenous artery and major side-branches are excised, leading to vascular insufficiency. In response to this injury, there is a time-dependent increase in limb perfusion and neovascularization that can be evaluated by laser Doppler blood flow (LDBF) analysis and by assessing capillary density in tissue sections. Development of collateral vessels is a complex process requiring the action of multiple genetic programs.[4] Microarray technology provides a method for identifying novel therapeutic and diagnostic target genes in cardiovascular disease, and this technology has been used previously to analyze the expression patterns of ≈12 000 transcripts involved in collateral vessel formation in C57BL/6 mice.[5]

Previous studies have found that ischemic hindlimb neovascularization is impaired in models of type 1 diabetes, including streptozatocin-treated rats and mice, nonobese diabetic mice, and alloxan-treated rabbits.[6–8] Type 2 diabetes is more prevalent in industrialized regions, and it is characterized by elevations in insulin and peripheral insulin resistance. Type 2 diabetes commonly occurs in patients who are obese and display features of the metabolic syndrome. The $Lepr^{db/db}$ mouse is a model of obesity and type 2 diabetes mellitus. $Lepr^{db/db}$ mice become identifiably obese and show elevations of plasma insulin and of blood glucose because of the spontaneous mutation of the leptin receptor.[9]

The current study had 2 aims. First, we tested whether a mouse model of obesity and type 2 diabetes ($Lepr^{db/db}$) displays impaired angiogenesis in hindlimbs that are made ischemic. Second, we performed DNA microarray analyses on $Lepr^{db/db}$ and wild-type (WT) mice before and after ischemic surgery to assess the differences in the expression profiles of angiogenesis-related proteins to identify candidates that may account for the impaired angiogenic response in $Lepr^{db/db}$ mice.

Methods

For the Methods section, please see the online supplement, available at http://atvb.ahajournals.org.

Results

Impaired Ischemia-Induced Vascular Remodeling in $Lepr^{db/db}$ Mice

The mice analyzed in this study were C57BL/6 (WT) and $Lepr^{db/db}$ on the C57BL/6 background. Blood pressure did not

Original received March 3, 2005; final version accepted May 11, 2005.

From the Molecular Cardiology/Whitaker Cardiovascular Institute, Boston University School of Medicine, Massachusetts.

Dr Schiekofer and Dr Galasso contributed equally to this work.

Correspondence to Dr Kenneth Walsh, PhD, Molecular Cardiology/Whitaker Cardiovascular Institute Boston University School of Medicine, 715 Albany St, W611 Boston, MA 02118. E-mail kxwalsh@bu.edu

Arterioscler Thromb Vasc Biol. **is available at http://www.atvbaha.org** **DOI: 10.1161/01.ATV.0000171994.89106.ca**

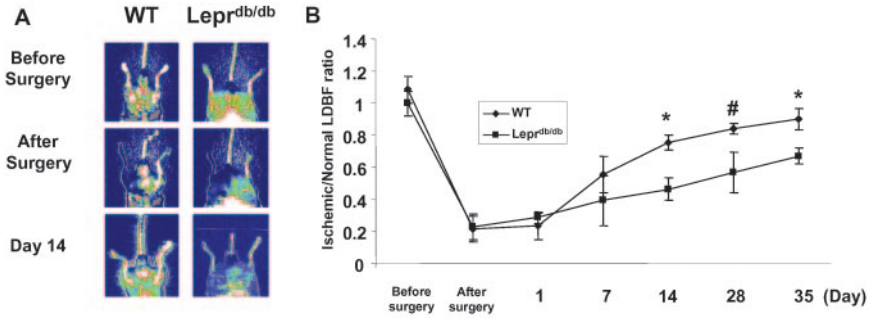

Figure 1. Impaired angiogenic response in the ischemic hindlimb of Lepr$^{db/db}$ mice compared with WT mice. A, Representative LDBF analyses in WT and Lepr$^{db/db}$ mice before surgery, immediately after surgery, and at 14 days after surgery. A low perfusion signal is indicated by dark blue, whereas a higher perfusion signal is indicated by white to red. B, Quantitative analysis of the ischemic/nonischemic LDBF ratio in WT and Lepr$^{db/db}$ mice before and after surgery and on postoperative days 1, 7, 14, 28, and 35 (n≥8); #$P<0.05$; *$P<0.01$.

differ between the 2 groups on the day of surgery (Table I, available online at http://atvb.ahajournals.org). Significant differences were observed in body weight, plasma glucose, and insulin and leptin levels between WT and Lepr$^{db/db}$ mice. All mice survived after surgical induction of left hindlimb ischemia. Figure 1A shows representative LDBF images of hindlimb blood flow before surgery, immediately after surgery, and at 14 days after surgery in the WT and Lepr$^{db/db}$ mice. Immediately after left femoral artery and vein resection, the ratio of blood flow between the ischemic and nonischemic hindlimbs decreased to 0.21±0.08 in WT and 0.22±0.08 in Lepr$^{db/db}$ mice, indicating that the severity of the induced ischemia was comparable in the 2 experimental groups. In WT mice, hindlimb blood flow perfusion increased to ≈75% of the nonischemic limb by day 14 (Figure 1B). In contrast, flow recovery in Lepr$^{db/db}$ mice was impaired, and the deficits in flow were statistically significant at 14, 28, and 35 days after surgery.

To investigate the extent of vascular remodeling at the level of the microcirculation in WT or Lepr$^{db/db}$ mice, quantitative analysis of capillary density in ischemic and contralateral adductor muscle of WT and Lepr$^{db/db}$ mice was determined in histological sections harvested on postoperative day 14. Quantitative analysis of CD31-positive cells revealed that the ischemia-induced increase in capillary density in the ischemic limb relative to the contralateral limb was essentially absent in Lepr$^{db/db}$ mice (Figure 2), indicative of an impaired angiogenic response in these animals. At the 14-day time point after surgery, the ischemic adductor muscle of Lepr$^{db/db}$ mice had significantly fewer CD31-positive cells compared with ischemic muscle from WT mice.

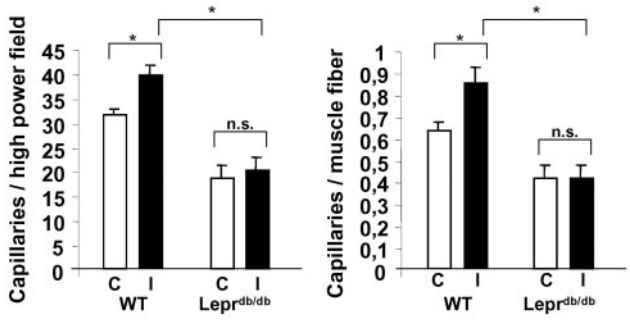

Figure 2. Reduced capillary density in ischemic Lepr$^{db/db}$ mice. Quantitative analysis of capillary density in ischemic (I) and contralateral (C) adductors of WT and Lepr$^{db/db}$ mice on postoperative day 14 (n=8). Capillary density was expressed as the number of capillaries per high-power field (×400; left) and capillaries per muscle fiber (right). *$P<0.01$.

Transcript Expression Before and After Hindlimb Ischemia in WT and Lepr$^{db/db}$ Mice

Transcript expression profiles in WT and Lepr$^{db/db}$ mice were analyzed before surgery and 1, 7, and 14 days after surgery. RNA was isolated from normal or ischemic adductor muscles and hybridized to Affymetrix GeneChip Mouse Expression Set microarray 2.0 (≈45 000 cDNAs and ESTs). Transcript level differences between WT and Lepr$^{db/db}$ mice at the same time point, or between different time points for the same mouse strain, were deemed statistically significant if the fold change difference was >2.0 (n=3; $P<0.01$). This analysis revealed 356 transcripts that were differentially regulated between WT and Lepr$^{db/db}$ mice before surgery. At 1, 7, and 14 days after surgery, 683, 3362, and 3128 transcripts, respectively, were differentially regulated compared with presurgery in WT mice. In Lepr$^{db/db}$ mice, 979, 310, and 1371 transcripts were differentially regulated at days 1, 7, and 14 respectively, compared with presurgery. Of note, many of the genes differentially expressed in Lepr$^{db/db}$ mice were not detected in the data set from WT mice. At the 14-day time point, 66% of genes detected as differentially expressed in Lepr$^{db/db}$ mice were not detected as differentially expressed in WT mice (Figure 3A). Similarly, 74% and 87% of differentially expressed transcripts in Lepr$^{db/db}$ mice were not detected as differentially expressed in WT mice at days 7 and 1 after surgery, respectively. Thus, although fewer genes are differentially expressed in Lepr$^{db/db}$ mice, they do not appear to simply represent a subset of genes regulated in WT. Instead, most of the transcripts regulated in Lepr$^{db/db}$ mice after ischemic surgery represent a different set of genes.

An automated analysis of related transcripts was performed using Ingenuity Pathways Analysis software. For this analysis, a set of 3128 transcripts differentially expressed in WT mice at day 14 compared with baseline (presurgery; fold change >2.0 or <2.0; $P<0.01$) was used as the starting point for generating biological networks. This time point was chosen because it was the earliest to achieve statistical significance in the LDBF analysis (Figure 1). One of the networks achieved a score of 27 and consisted of 35 transcripts, of which 34 were differentially regulated at 14 days after surgery (Figure 3B). A key providing transcript identity for this network and its fold change is provided in Table 1. These transcripts included the angiogenesis-regulatory factors vascular endothelial growth factor-A (VEGF-A),

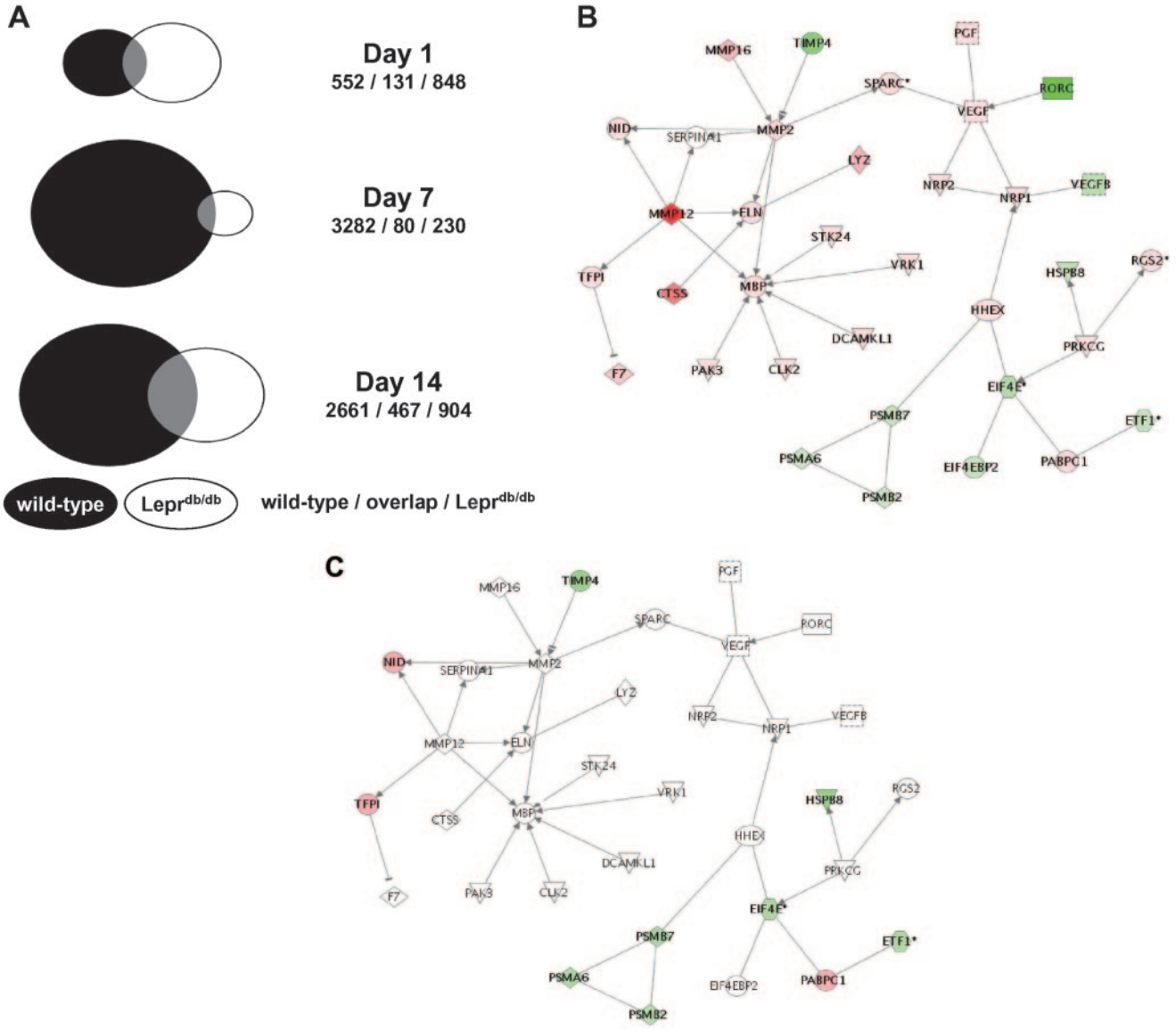

Figure 3. Biological network analysis of differentially expressed transcripts in WT and Lepr$^{db/db}$ mice. A, Venn diagrams representing the sets of transcripts in WT and Lepr$^{db/db}$ mice that are differentially regulated at 1, 7, and 14 days after surgery. Black represents transcripts differentially regulated in WT; white, transcripts differentially regulated in Lepr$^{db/db}$; gray, transcripts differentially regulated in both strains. B, Network constructed from differentially regulated transcripts comparing microarray data from the hindlimbs of WT mice at baseline and 14 days after surgery. The network score was 27. Shaded genes were identified as differentially expressed by the extent of shading that is indicative of the magnitude of regulation. Red shading indicates upregulation at day 14 relative to baseline, whereas green shading indicates downregulation. Node shapes indicate function; diamond, an enzyme; square, growth factor; triangle, kinase; circle, other. Asterisk indicates transcripts identified multiple times on the microarray; line, physical interactions (eg, formation of complexes); arrow, functional interaction (activation); ⊣, functional interaction (inhibition). C, Transcripts differentially regulated in Lepr$^{db/db}$ mice comparing baseline and day 14 after surgery superimposed on the network constructed for WT mice as described in B.

neuropilin-1, neuropilin-2, placental growth factor, and the putative transcriptional regulators of neuropilin-1, the HHEX homeobox factor.[10] In contrast to the identification that a number of proangiogenic transcripts were upregulated, VEGF-B and RORC, a transcriptional regulator of VEGF-A,[11] were downregulated. Other differentially expressed transcripts in this network included 3 proteasome subunits, translation regulatory factors (EIF4E, EIF4EBP2, and ETFI), the proteases cathepsin S and lysozyme, and a number of metalloproteinases (matrix metalloproteinase-2 [MMP2], MMP12, MMP16). In addition, the matrix proteins elastin, SPARC, and myelin basic protein (MBP), and 5 protein kinases that phosphorylate MBP, were upregulated in the ischemic hindlimbs of WT mice. Once established, the 1371 transcripts differentially expressed in Lepr$^{db/db}$ mice at day 14 were superimposed on this network (Figure 3C; Table II, available online at http://atvb.ahajournals.org). Only 10 differentially regulated transcripts were observed in Lepr$^{db/db}$ mice compared with 34 in WT mice. Of note, differentially regulated transcripts observed in WT but not in Lepr$^{db/db}$ mice included the angiogenesis growth factors and neuropilin coreceptors elastin and the MMPs.

A number of transcripts within the network were also identified as differentially regulated at earlier time points. In

TABLE 1. Pathways Analysis Network for WT Mice on Day 14 After Surgery Compared With Baseline ($P<0.01$)

Transcript Symbol	Transcript Name	Fold Change
CLK2	CDC-like kinase 2	2.5
CTSS	Cathepsin S	22.1
DCAMKL1	Doublecortin and CaM kinase-like 1	4.3
EIF4E	Eukaryotic translation initiation factor 4E	−3.1
EIF4EBP2	Eukaryotic translation initiation factor 4E binding protein 2	−2.3
ELN	Elastin	5.1
ETF1	Eukaryotic translation termination factor 1	−2.4
F7	Coagulation factor VII	8.2
HHEX	Hematopoietically expressed homeobox	4.6
HSPB8	Heat shock 22-kDa protein 8	−2.5
LYZ	Lysozyme	11.7
MBP	Myelin basic protein	5.9
MMP2	Matrix metalloproteinase 2	6.2
MMP12	Matrix metalloproteinase 12	92.9
MMP16	Matrix metalloproteinase 16	11.4
NID	Nidogen	3.4
NRP1	Neuropilin-1	2.1
NRP2	Neuropilin-2	4.7
PABPC1	Poly(A) binding protein, cytoplasmic 1	2.2
PAK3	P21 (CDKN1A)-activated kinase 3	3.9
PGF	Placental growth factor, VEGF-related protein	5.9
PRKCG	Protein kinase C, γ	3.1
PSMA6	Proteasome (prosome, macropain) subunit, α-type, 6	−2.0
PSMB2	Proteasome (prosome, macropain) subunit, β-type, 2	−2.1
PSMB7	Proteasome (prosome, macropain) subunit, β-type, 7	−2.1
RGS2	Regulator of G-protein signaling 2	3.2
RORC	RAR-related orphan receptor C	−7.7
SPARC	Secreted protein, acidic, cysteine-rich (osteonectin)	3.1
STK24	Serine/threonine kinase 24	2.4
TFPI	Tissue factor pathway inhibitor	2.4
TIMP4	Tissue inhibitor of metalloproteinase-4	−5.4
VEGF-A	Vascular endothelial growth factor A	3.5
VEGF-B	Vascular endothelial growth factor B	−2.8
VRK1	Vaccinia-related kinase 1	2.2

WT mice, ELN, NRP1, and EIF4E were detected as differentially regulated at day 1 after surgery, and CLK2, CTSS, EIF4E, EIF4EBP2, HHEX, HSPB8, LYZ, MBP, MMP16, NID, NRP1, NRP2, PAK3, PSMB7, RGS2, RORC, SPARC, tissue factor pathway inhibitor, tissue inhibitor of metalloproteinases-4 (TIMP4), VEGF-A, and VRK1 were detected as differentially regulated at 7 days. In contrast, in Lepr$^{db/db}$ mice, only RGS2 was identified as differentially regulated at 1 day, and MBP and TIMP4 were identified as differentially regulated at 7 days.

The 356 transcripts identified as differentially expressed between WT and Lepr$^{db/db}$ mice before surgery (fold change >2.0 or <2.0; $P<0.01$) were superimposed on this network (data not shown). No differentially expressed transcripts were observed in the network, demonstrating that the differences observed between WT and Lepr$^{db/db}$ mice reflected a differential response of the tissues to ischemic injury rather than a baseline difference presurgery. Finally, other networks were identified using the Ingenuity software (Please see online supplement, available at http://atvb.ahajournals.org).

Quantitative RT-PCR of Selected Transcripts

The differential expression of 3 angiogenesis-related transcripts identified by the microarray and pathway analyses were examined in greater detail by quantitative RT-PCR (QRT-PCR) using the primer sets listed in supplemental Table III (available online at http://atvb.ahajournals.org). The representative transcripts chosen for this analysis were elastin, the main component of the extracellular matrix of arteries, neuropilin-1, a coreceptor for VEGF receptor 2 (VEGF-R2),[12] and VEGF-A, a major angiogenic factor. Consistent with the microarray data, little or no difference in the levels of these transcripts were apparent before surgery in the limbs of WT and Lepr$^{db/db}$ mice (Table 2). QRT-PCR assays showed that these transcripts were upregulated at 1, 7, and 14 days after surgery (elastin and neuropilin-1) or at 7 and 14 days after surgery (VEGF-A) in WT mice. However, elastin, neuropilin-1, or VEGF-A upregulation was not observed in the Lepr$^{db/db}$ mice on days 1, 7, or 14 after surgery, consistent with the findings of the microarray data.

Elastin and Neuropilin-1 Protein Expression in Ischemic Muscle After Hindlimb Ischemia

Elastin and neuropilin-1, 2 factors involved in arterial morphogenesis or angiogenesis, were also analyzed by Western immunoblot analysis in WT and Lepr$^{db/db}$ mice. Elastin and neuropilin-1 transcripts were identified as differentially expressed at 1, 7, and 14 days in WT but not Lepr$^{db/db}$ mice. Immunoblotting for elastin in samples from muscle tissue of Lepr$^{db/db}$ and WT mice before hindlimb ischemia surgery and on days 1, 7, and 14 after surgery showed an upregulation in WT mice, whereas no upregulation was detected in the ischemic limbs of Lepr$^{db/db}$ mice (Figure 4A). Immunoblotting also revealed an increase in the neuropilin-1 content of the ischemic muscle tissue in WT mice after hindlimb ischemia, in accordance with the microarray and QRT-PCR data. In contrast, the increase in neuropilin-1 protein content after ischemic muscle tissue of Lepr$^{db/db}$ mice was considerably lower (Figure 4B).

Discussion

Diabetes and obesity promote microvascular rarefaction and diminish collateral vessel development in the heart and peripheral tissues.[1,2] The Lepr$^{db/db}$ mouse is a model of type 2 diabetes that results from a leptin receptor deficiency. Here we show that the angiogenic repair of ischemic hindlimbs is impaired in Lepr$^{db/db}$ mice compared with C57BL/6 (WT) mice, as evaluated by laser Doppler flow and capillary density analyses. These data are consistent with observations of diminished skin wound healing in these animals.[13–15]

Here it is also shown that the impairment is associated with alterations in a gene regulatory network involved in the physiological revascularization process. Microarray analysis revealed alterations in the expression patterns of numerous

TABLE 2. Comparison of Microarray and QRT-PCR Data*

Transcript	Analysis**	WT/db Before Injury	WT 1/0	WT 7//0	WT 14/0	db 1/0	db 7/0	db 14/0
Elastin	Microarray	0.9	3.2†	1.6	5.1†	−2.0	−1.9	−1.3
	QRT-PCR	0.8	2.5†	2.9†	3.2†	1.1	−1.2	−1.7
Neuropilin-1	Microarray	1.0	3.0†	3.0†	2.1†	1.7	1.5	1.1
	QRT-PCR	1.2	4.2†	3.8†	3.0†	1.3	1.9	1.4
VEGF-A	Microarray	1.3	1.2	3.2†	3.5†	−1.5	−1.4	−1.2
	QRT-PCR	1.1	−1.2	2.4†	2.9†	−2.1†	−2.0	−1.7

*Values represent fold change comparing WT and Lepr$^{db/db}$ mice before injury or fold change at 1, 7, or 14 days relative to before injury for WT or Lepr$^{db/db}$ mice; **all analysis values represent SEM performed in triplicates.
†$P<0.01$.

extracellular matrix protein–related and angiogenic growth factor–related transcripts between WT and Lepr$^{db/db}$ mice after hindlimb ischemia. In particular, factors underexpressed in the ischemic limbs of Lepr$^{db/db}$ mice at 14 days after ischemia include the angiogenic factors VEGF-A (confirmed by QRT-PCR), placental growth factor, neuropilin-1 (confirmed by QRT-PCR and Western immunoblot), neuropilin-2, and elastin (confirmed by QRT-PCR and Western immunoblot). None of the transcripts identified in this network were found to be differentially expressed between these 2 mouse lines at baseline (data not shown). These data indicate that the Lepr$^{db/db}$ mouse fails to correctly activate a multifaceted angiogenic program in response to ischemic injury.

Analysis of the microarray data reveals that fewer transcripts are differentially expressed in the ischemic limbs of Lepr$^{db/db}$ mice than WT mice at days 7 and 14 after surgery. Comparison of the data sets indicate that most of the genes identified as differentially regulated in Lepr$^{db/db}$ mice do not represent a subset of the genes regulated in WT mice. Instead, the majority of transcripts represent a distinct set of genes that are differentially regulated in WT and Lepr$^{db/db}$ mice. In this regard, leptin has been recognized as a proangiogenic molecule that displays synergistic effects with fibroblast growth factor-2 and VEGF in promoting blood vessel growth.[16,17] Although leptin deficiency may be directly responsible for some of the changes in the angiogenic program of Lepr$^{db/db}$ mice, the diabetes and obesity that develop as a consequence of leptin deficiency is also likely to have a profound impact on the angiogenesis-regulatory network in this model.

Our experiments showed that transcripts for MMP2, MMP12, or MMP16 were upregulated in WT mice after hindlimb ischemia, but this response was suppressed in Lepr$^{db/db}$ mice. These data also revealed the downregulation of TIMP4, a negative regulator of MMP2, in WT and Lepr$^{db/db}$ mice. Metalloproteinases hydrolyze components of the extracellular matrix, creating the cellular environments required during development or morphogenesis.[18] MMPs are important regulators of angiogenesis by virtue of their abilities to allow endothelial cell migration through the degradation of matrix and to activate latent cytokines and growth factors. In this regard, MMP2 cleaves SPARC, a protein implicated in tumor progression and angiogenesis,[19,20] and it has been proposed that SPARC cleavage can yield proangiogenic peptides.[21] Like MMP2, SPARC transcripts are upregulated in the ischemic limbs of WT but not Lepr$^{db/db}$ mice. Less is known about the proangiogenic activities of MMP12 and MMP16, but MMP12 has been implicated in macrophage migration,[22] and MMP16 promotes the cleavage and activation of MMP2.[23]

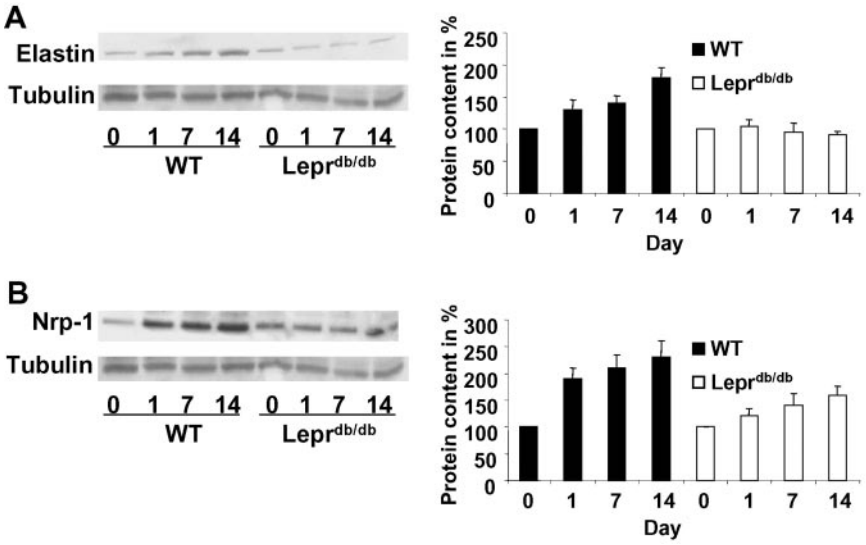

Figure 4. Immunoblot analysis of neuropilin-1 and elastin expression in WT and Lepr$^{db/db}$ mice. Western immunoblots with the indicated antibodies were performed on adductor muscle before surgery and at 1, 7, and 14 days after surgery. Representative immunoblots for elastin (A, left panel) and neuropilin-1 (B, left panel) in WT and Lepr$^{db/db}$ mice are shown. Quantitative analysis of relative changes in elastin (A, right panel) and neuropilin-1 (B, right panel). Elastin and neuropilin-1 signals were normalized to the signal for tubulin and expressed as percent relative to control (before surgery).

The microarray, QRT-PCR, and Western immunoblot analyses revealed upregulation of elastin in WT but not Lepr$^{db/db}$ mice. Elastin is the main component of the extracellular matrix of arteries, and it performs a regulatory function during arterial morphogenesis and development by controlling proliferation of smooth muscle and stabilizing the arterial structure.[24] In diabetic animals, the elasticity of this protein is reduced as a result of increased glycosylation, leading to the accumulation and reorganization of smooth muscle cells.[25] In addition, the involvement of elastin derived peptides in angiogenesis has been reported.[26] These proangiogenic fragments of elastin can be produced by the proteolytic actions of MMPs, including MMP2. Elastin is also cleaved by cathepsin S and MMP12,[27,28] which are upregulated in the ischemic hindlimbs of WT but not Lepr$^{db/db}$ mice.

In addition to the dysregulation of extracellular matrix, impaired regulation of a number of angiogenic growth factors and growth factor receptors were differentially regulated in the ischemic limbs of WT and Lepr$^{db/db}$ mice. Microarray data showed that VEGF-A, placental growth factor, neuropilin-1, and neuropilin-2 were upregulated in WT mice after surgery, but this regulation was impaired in Lepr$^{db/db}$ mice. VEGF-A is a key hypoxia-inducible angiogenic factor that induces the proliferation, migration, and survival of endothelial cells,[29] and also promotes the expression of proteases implicated in pericellular matrix degradation in angiogenesis.[30] Activation of VEGF-R1 by either VEGF-A or placental growth factor induces different gene expression profiles and promotes the phosphorylation of distinct tyrosine residues in the tyrosine kinase domain of VEGF-R1, and the combined administration of these factors enhances VEGF driven angiogenesis.[31] Neuropilin-1 and neuropilin-2 are cell-surface glycoproteins that participate in the regulation of angiogenesis.[32] Neuropilin-1 functions as a coreceptor for VEGF-R2 that enhances the activity of VEGF-A in ischemic tissues.[12]

An unexpected finding of this study is the observation that MBP and a series of protein kinases that phosphorylate this protein are upregulated in the ischemic limbs of WT but not Lepr$^{db/db}$ mice. MBP is also cleaved by MMP2.[33] MBP functions in maintaining the structural integrity of the myelin sheath, and it is subjected to a wide array of post-translational modifications.[34] Thus, the impaired induction of MBP and its regulatory network in Lepr$^{db/db}$ mice may contribute to the peripheral neuropathy that is associated with peripheral vascular disease.[35]

There has been considerable interest in "therapeutic angiogenesis" because many patients are not amenable to traditional forms of revascularization.[36] However, despite a large number of positive preclinical studies, the results of controlled therapeutic angiogenesis trials have been largely negative. One reason that may account for the lack of clinical success is that preclinical studies are almost exclusively performed on healthy, young animals that exhibit robust angiogenic responses, whereas the patient population experiences a high incidence of obesity and insulin-resistant diabetes. Therefore, we used a mouse model of type 2 diabetes and obesity to study revascularization after ischemic injury. Lepr$^{db/db}$ mice displayed functional and anatomic deficits in hindlimb revascularization that was associated with the dysregulation of a complex angiogenesis-regulatory network. These data suggest that a single angiogenic agent may not be sufficient to effectively stimulate angiogenesis in subjects with insulin-resistant diabetes and that the control of obesity and its associated diseases may improve the success of proangiogenic therapies.

Acknowledgments

This work was supported by National Heart, Lung, and Blood Institute grant N01-HV-28178 from the National Institutes of Health and National Institutes of Health grants HL66957, AR40197, AG15052, and AG17241 to K.W. We acknowledge the technical assistance of A. Bialik.

References

1. Adeghate E. Molecular and cellular basis of the etiology and management of diabetic cardiomyopathy: a short review. *Mol Cell Biochem*. 2004;261:187–191.
2. Federman DG, Bravata DM, Kirsner RS. Peripheral arterial disease. A systemic disease extending beyond the affected extremity. *Geriatrics*. 2004;59:26, 29–30.
3. Couffinhal T, Silver M, Zheng LP, Kearney M, Witzenbichler B, Isner JM. A mouse model of angiogenesis. *Am J Pathol*. 1998;152:1667–1679.
4. Carmeliet P. Mechanisms of angiogenesis and arteriogenesis. *Nat Med*. 2000;6:389–395.
5. Lee CW, Stabile E, Kinnaird T, Shou M, Devaney JM, Epstein SE, Burnett MS. Temporal patterns of gene expression after acute hindlimb ischemia in mice: insights into the genomic program for collateral vessel development. *J Am Coll Cardiol*. 2004;43:474–482.
6. Rivard A, Silver M, Chen D, Kearney M, Magner M, Annex B, Peters K, Isner JM. Rescue of diabetes-related impairment of angiogenesis by intramuscular gene therapy with adeno-VEGF. *Am J Pathol*. 1999;154:355–363.
7. Roguin A, Nitecki S, Rubinstein I, Nevo E, Avivi A, Levy N, Abassi Z, Sabo E, Lache O, Frank M, Hoffman A, Levy A. Vascular endothelial growth factor (VEGF) fails to improve blood flow and to promote collateralization in a diabetic mouse ischemic hindlimb model. *Cardiovasc Diabetol*. 2003;2:18.
8. Schratzberger P, Walter DH, Rittig K, Bahlmann FH, Pola R, Curry C, Silver M, Krainin JG, Weinberg DH, Ropper AH, Isner JM. Reversal of experimental diabetic neuropathy by VEGF gene transfer. *J Clin Invest*. 2001;107:1083–1092.
9. Chen H, Charlat O, Tartaglia LA, Woolf EA, Weng X, Ellis SJ, Lakey ND, Culpepper J, Moore KJ, Breitbart RE, Duyk GM, Tepper RI, Morgenstern JP. Evidence that the diabetes gene encodes the leptin receptor: identification of a mutation in the leptin receptor gene in db/db mice. *Cell*. 1996;84:491–495.
10. Minami T, Murakami T, Horiuchi K, Miura M, Noguchi T, Miyazaki J, Hamakubo T, Aird WC, Kodama T. Interaction between hex and GATA transcription factors in vascular endothelial cells inhibits flk-1/KDR-mediated vascular endothelial growth factor signaling. *J Biol Chem*. 2004;279:20626–20635.
11. Wang H, Chu W, Das SK, Zheng Z, Hasstedt SJ, Elbein SC. Molecular screening and association studies of retinoid-related orphan receptor gamma (RORC): a positional and functional candidate for type 2 diabetes. *Mol Genet Metab*. 2003;79:176–182.
12. Soker S, Takashima S, Miao HQ, Neufeld G, Klagsbrun M. Neuropilin-1 is expressed by endothelial and tumor cells as an isoform-specific receptor for vascular endothelial growth factor. *Cell*. 1998;92:735–745.
13. Jacobi J, Jang JJ, Sundram U, Dayoub H, Fajardo LF, Cooke JP. Nicotine accelerates angiogenesis and wound healing in genetically diabetic mice. *Am J Pathol*. 2002;161:97–104.
14. Galeano M, Altavilla D, Cucinotta D, Russo GT, Calo M, Bitto A, Marini H, Marini R, Adamo EB, Seminara P, Minutoli L, Torre V, Squadrito F. Recombinant human erythropoietin stimulates angiogenesis and wound healing in the genetically diabetic mouse. *Diabetes*. 2004;53:2509–2517.
15. Galeano M, Deodato B, Altavilla D, Cucinotta D, Arsic N, Marini H, Torre V, Giacca M, Squadrito F. Adeno-associated viral vector-mediated human vascular endothelial growth factor gene transfer stimulates angiogenesis and wound healing in the genetically diabetic mouse. *Diabetologia*. 2003;46:546–555.

16. Cao R, Brakenhielm E, Wahlestedt C, Thyberg J, Cao Y. Leptin induces vascular permeability and synergistically stimulates angiogenesis with FGF-2 and VEGF. *Proc Natl Acad Sci U S A*. 2001;98:6390–6395.
17. Suganami E, Takagi H, Ohashi H, Suzuma K, Suzuma I, Oh H, Watanabe D, Ojima T, Suganami T, Fujio Y, Nakao K, Ogawa Y, Yoshimura N. Leptin stimulates ischemia-induced retinal neovascularization: possible role of vascular endothelial growth factor expressed in retinal endothelial cells. *Diabetes*. 2004;53:2443–2448.
18. Visse R, Nagase H. Matrix metalloproteinases and tissue inhibitors of metalloproteinases: structure, function, and biochemistry. *Circ Res*. 2003; 92:827–839.
19. Lane TF, Iruela-Arispe ML, Sage EH. Regulation of gene expression by SPARC during angiogenesis in vitro. Changes in fibronectin, thrombospondin-1, and plasminogen activator inhibitor-1. *J Biol Chem*. 1992;267:16736–16745.
20. St Croix B, Rago C, Velculescu V, Traverso G, Romans KE, Montgomery E, Lal A, Riggins GJ, Lengauer C, Vogelstein B, Kinzler KW. Genes expressed in human tumor endothelium. *Science*. 2000;289:1197–1202.
21. Lane TF, Iruela-Arispe ML, Johnson RS, Sage EH. SPARC is a source of copper-binding peptides that stimulate angiogenesis. *J Cell Biol*. 1994; 125:929–943.
22. Anghelina M, Schmeisser A, Krishnan P, Moldovan L, Strasser RH, Moldovan NI. Migration of monocytes/macrophages in vitro and in vivo is accompanied by MMP12-dependent tunnel formation and by neovascularization. *Cold Spring Harb Symp Quant Biol*. 2002;67:209–215.
23. Miyamori H, Takino T, Kobayashi Y, Tokai H, Itoh Y, Seiki M, Sato H. Claudin promotes activation of pro-matrix metalloproteinase-2 mediated by membrane-type matrix metalloproteinases. *J Biol Chem*. 2001;276: 28204–28211.
24. Karnik SK, Brooke BS, Bayes-Genis A, Sorensen L, Wythe JD, Schwartz RS, Keating MT, Li DY. A critical role for elastin signaling in vascular morphogenesis and disease. *Development*. 2003;130:411–423.
25. Seyama Y, Wachi H. Atherosclerosis and matrix dystrophy. *J Atheroscler Thromb*. 2004;11:236–245.
26. Robinet A, Fahem A, Cauchard JH, Huet E, Vincent L, Lorimier S, Antonicelli F, Soria C, Crepin M, Hornebeck W, Bellon G. Elastin-derived peptides enhance angiogenesis by promoting endothelial cell migration and tubulogenesis through upregulation of MT1-MMP. *J Cell Sci*. 2005;118:343–356.
27. Chapman HA, Riese RJ, Shi GP. Emerging roles for cysteine proteases in human biology. *Annu Rev Physiol*. 1997;59:63–88.
28. Sternlicht MD, Werb Z. How matrix metalloproteinases regulate cell behavior. *Annu Rev Cell Dev Biol*. 2001;17:463–516.
29. Ferrara N, Gerber HP, LeCouter J. The biology of VEGF and its receptors. *Nat Med*. 2003;9:669–676.
30. Mandriota SJ, Seghezzi G, Vassalli JD, Ferrara N, Wasi S, Mazzieri R, Mignatti P, Pepper MS. Vascular endothelial growth factor increases urokinase receptor expression in vascular endothelial cells. *J Biol Chem*. 1995;270:9709–9716.
31. Park JE, Chen HH, Winer J, Houck KA, Ferrara N. Placenta growth factor: potentiation of vascular endothelial growth factor bioactivity, in vitro and in vivo, and high affinity binding to Flt-1 but not to Flk-1/KDR. *J Biol Chem*. 1994;269:25646–25654.
32. Miao HQ, Lee P, Lin H, Soker S, Klagsbrun M. Neuropilin-1 expression by tumor cells promotes tumor angiogenesis and progression. *FASEB J*. 2000;14:2532–2539.
33. Siebert H, Dippel N, Mader M, Weber F, Bruck W. Matrix metalloproteinase expression and inhibition after sciatic nerve axotomy. *J Neuropathol Exp Neurol*. 2001;60:85–93.
34. Harauz G, Ishiyama N, Hill CM, Bates IR, Libich DS, Fares C. Myelin basic protein-diverse conformational states of an intrinsically unstructured protein and its roles in myelin assembly and multiple sclerosis. *Micron*. 2004;35:503–542.
35. Parkhouse N, Le Quesne PM. Impaired neurogenic vascular response in patients with diabetes and neuropathic foot lesions. *N Engl J Med*. 1988;318:1306–1309.
36. de Muinck ED, Simons M. Re-evaluating therapeutic neovascularization. *J Mol Cell Cardiol*. 2004;36:25–32.

Arteriosclerosis, Thrombosis, and Vascular Biology

JOURNAL OF THE AMERICAN HEART ASSOCIATION

Impaired Revascularization in a Mouse Model of Type 2 Diabetes Is Associated With Dysregulation of a Complex Angiogenic-Regulatory Network

Stephan Schiekofer, Gennaro Galasso, Kaori Sato, Benjamin J. Kraus and Kenneth Walsh

Arterioscler Thromb Vasc Biol. 2005;25:1603-1609; originally published online May 26, 2005;
doi: 10.1161/01.ATV.0000171994.89106.ca
Arteriosclerosis, Thrombosis, and Vascular Biology is published by the American Heart Association, 7272 Greenville Avenue, Dallas, TX 75231

Print ISSN: 1079-5642. Online ISSN: 1524-4636

Methods

Materials

Neuropilin-1 and elastin antibodies were purchased from Santa Cruz Biotechnology (Santa Cruz, CA, USA). Tubulin antibody was purchased from Oncogene (Cambridge, MA, USA).

Mouse model

$Lepr^{db/db}$ mice in a C57/BL6 background and wild-type (WT) C57/BL6 mice purchased from the Jackson Laboratory were used for this study. Study protocols were approved by the Institutional Animal Care and Use Committee in Boston University. Mice were subjected to unilateral hind limb surgery under anesthesia with sodium pentobarbital (50 mg/kg intraperitoneally). An incision was made in the skin overlying the middle portion of the left hind limb. After ligation of the proximal end of the femoral artery and the distal portion of the saphenous artery, the artery and side-branches were dissected free and excised.[1, 2] Before surgery body weight (BW) and systolic blood pressure (sBP) were determined using a tail-cuff pressure analysis system in the conscious state.

Laser Doppler blood flow analysis

Hind limb blood flow was measured using a laser Doppler blood flow (LDBF analyzer (Moor LDI; Moor Instruments, Devon, United Kingdom). Immediately before surgery and on postoperative days 1, 7, 14, 28 and 35, LDBF analysis were performed on legs and feet. Blood flow was displayed as changes in the laser frequency using different color pixels. After scanning, stored images were analyzed to quantify blood flow. To avoid

data variations, hind limb blood flow was expressed as the ratio of left (ischemic) to right (nonischemic) limb.

Serum measurement

Blood samples were collected on the day of surgery. Glucose was measured with an enzymatic kit (Wako Chemicals, Richmond, VA, USA), leptin levels were measured with a Mouse Leptin ELISA kit (Crystal CHEM INC, Downers Grove, IL, USA) and insulin levels were assayed with an EIA kit (Wako Chemicals, Richmond, VA, USA).

Tissue preparation and immunohistochemistry

The mice were sacrificed at time points before or after surgery with an overdose of sodium pentobarbital. For total protein or RNA extraction, isolated tissue samples were rinsed in phosphate-buffered saline (PBS) to remove excess blood, snap-frozen in liquid nitrogen, and stored at -80 °C until use. For immunohistochemistry, muscle samples were imbedded in OCT compound (Miles, Elkhart, IN, USA) and snap-frozen in liquid nitrogen. Tissue slices (5 μm in thickness) were prepared and immunohistochemistry was performed using antibodies for CD31 (PECAM-1: Becton Dickinson, Franklin Lakes, NJ, USA). Capillary density within the adductor muscle was quantified by histological analysis. Fifteen randomly chosen microscopic fields from three different sections in each tissue block were examined for the presence of capillary endothelial cells for each mouse specimen. Capillary density was expressed as the number of CD-31-positive features per high power field (x 400) and the number of capillaries per muscle fiber.

Preparation of cRNA for microarray analysis

Adductor muscle in the ischemic limb was placed in TRizol (Ultraspec™-II RNA Isolation System, Biotecx, USA) and homogenized to extract total RNA according to the manufacturer's recommendations. RNA was resuspended in DEPC treated H_2O and further purified using RNATAckTmResin (Ultraspec™-II RNA Isolation System, Biotecx, USA) according to the manufacturer's instructions. After purification, an aliquot was electrophoresed in a 2.0% agarose gel and visualized by staining with ethidium bromide to confirm the absence of significant degradation. These samples were used to generate cDNA using poly-dT primer incorporating T7 promoter in the Superscript system (Invitrogen) according to the Affymetrix protocol (Affymetrix, Santa Clara, CA). Resulting cDNA was used to generate labeled cRNA by incorporating biotinylated CTP and UTP using the ENZO Bioarray High Yield transcript labeling kit (Affymetrix). cRNA (20 µg) was fragmented in fragmentation buffer (40 mM Tris (pH 8.1), 100 mM potassium acetate, 30 mM magnesium acetate) for 35 min at 94 C. Subsequently samples and hybridization controls were hybridized to Affymetrix GeneChip® Mouse Expression Set 430 microarrays 2.0 for 16 hours at 45 °C. The microarrays were washed and stained with strepavidin-phycoerythrin, washed and incubated with anti-streptavidin antibody twice, and finally washed according to the manufacturer's instructions. The arrays were then scanned at 488 nm using G25000A gene array scanner (Agilent, Palo Alto, CA). Gene expression data was obtained for adductor muscle in the ischemic limb from $Lepr^{db/db}$ mice and wild type mice at each of 4 time points (before hind limb ischemia, 1 day, 7 days and 14 days after hind limb ischemia surgery). Three independent experimental replicates of each condition for each time point were performed.

Data quantification, normalization and analysis

Following data acquisition, the scanned images were quantified using MAS 5.0 software (Affymetrix) yielding a signal intensity for each probe on the GeneChip. The signal intensities from the probes for each transcript were then used to determine an overall expression level, a detection confidence score, and a present / absent call according to algorithms implemented in MAS 5.0 software. The arrays were then linearly scaled to an average expression level of 500 units on each chip in MAS 5.0. For each transcript, fold change and statistical significance of differential expression were calculated. Fold change was calculated using the average signal from each experimental group. Statistical significance was calculated using two methods; a standard two-factor (strain, time point) ANOVA and a one-factor (time point) ANOVA implemented in the NIA Array Analysis Tool (http://cgd.rrc.uic.edu/anova/) using a Bayesian estimate of the variance between replicates. ANOVA p-values were corrected for multiple hypothesis testing using the method of Benjamini and Hochberg.[3] Each transcript was annotated based on a download of the NetAffx database (Affymetrix, Santa Clara, CA).

An automated analysis of related transcripts was performed using Ingenuity Pathways Analysis, a web-delivered application that evaluates biological networks (www.ingenuity.com). For this analysis a set of 3129 gene identifiers revealed as significantly changed in WT mice on day 14 compared to baseline (pre-surgery) (fold change >/<2.0, $p<0.01$) was mapped to its corresponding gene object in the Ingenuity Pathways Knowledge Base that is derived from information in the scientific literature. These Focus Genes were then used for generating biological networks based upon the identities of the Focus Genes and interactions with genes/proteins that are reported in

the literature. The software computes a score for each network according to the fit of the Focus Genes that were significantly changed in Lepr$^{db/db}$ and WT mice between 14 days and pre-surgery using a Fischer's exact test. The score is derived from a p-value and indicates the likelihood of the Focus Genes in a network being found together due to random chance. A score of 2 indicates that there is a 1% chance that the Focus Genes are together in a network due to random chance. Therefore, scores of ≥2 have ≥99% confidence (and ≥3 have ≥99.9%) of not being generated by random chance alone.

QRT-PCR analysis

Total RNA was isolated and purified from the ischemic muscle in the ischemic limb as described above by RNA-TRIZOL extraction (Ultraspec™-II RNA Isolation System, Biotecx, USA). RNA (2 µg) was treated (30 min at 37 °C) with amplification grade DNase 1 (Invitrogen, USA) following phenol/chloroform extraction (1:1). cDNA was produced using Taqman reverse transcription (Invitrogen, USA) kits. Real-time polymerase chain reaction (QRT-PCR) was performed in triplicate on ABI-Prism 7900 using SYBR Green I as a double stranded DNA specific dye according to manufacturer's instruction (PE-Applied Biosystems, Great Britain) using SYBR® Green PCR Master Mix (1:1, PE-Applied Biosystems, Great Britain), forward and reverse primers (200 nM each), and sample cDNA. The appropriate primers were obtained from Integrated DNA Technologies, USA. Primers were designed to be compatible with a single QRT-PCR thermal profile (95 °C for 10 min, and 40 cycles of 95 °C for 30 s and 60 °C for 1 min) such that multiple transcripts could be analyzed simultaneously. Accumulation of PCR product was monitored in real time (PE-Applied Biosystems), and the crossing threshold (Ct) was determined using the PE-Applied Biosystems software.

For each set of primers, a no template control and a no reverse amplification control were included. Postamplification dissociation curves were performed to verify the presence of a single amplification product in the absence of DNA contamination. Fold changes in transcript expression were determined using the Ct method. To standardize the quantitation of the selected transcripts, glyceraldehydes-3-phosphate dehydrogenase (GAPDH) from each sample was quantified by QRT-PCR and the selected transcripts were normalized to GAPDH. Data of QRT-PCR analysis are shown as the means ± S.E. of mean. All data were evaluated with a two-tailed, unpaired Student's t test or compared by one-way analysis of variance ($p<0.01$).

Western Blot Analysis

Tissue samples obtained before surgery and at days 1, 7 and 14 post-surgery were removed, snap frozen, and crushed under liquid nitrogen before tissue was homogenized in cold lysis buffer containing 20 mM Tris-HCL (pH 8.0), 1% NP-40, 150 mM NaCl, 0.5% deoxycholic acid, 1 mM sodium orthovanadate, 1 µg/ml leupeptin, 1 µg/ml aprotinin and 1 mg/ml Pefabloc SC Plus (Roche). Proteins (50 µg) were separated by SDS-PAGE on 10% separation gels and transferred to nitrocellulose membranes by semidry transfer. Following transfer to membranes, immunoblot analysis was performed with the indicated antibodies neuropilin-1 (Santa Cruz Biotechnology, USA) and elastin (Santa Cruz Biotechnology, USA) at a 1:200 dilution. This was followed by incubation with secondary antibody conjugated with horseradish peroxidase (HRP) at a 1:2000 dilution. ECL-PLUS Western Blotting Detection kit (Amersham Pharmacia Biotech, Piscataway, New Jersey, USA) was used for detection. The relative

changes in neuropilin-1 or elastin were normalized to the tubulin signal and expressed as percent relative to control.

Reference

1. Couffinhal T, Silver M, Zheng LP, Kearney M, Witzenbichler B, Isner JM. A mouse model of angiogenesis. *Am. J. Pathol.* 1998;152:1667-1679.

2. Shibata R, Ouchi N, Kihara S, Sato K, Funahashi T, Walsh K. Adiponectin stimulates angiogenesis in response to tissue ischemia through stimulation of amp-activated protein kinase signaling. *J. Biol. Chem.* 2004;279:28670-28674.

3. Benjamini Y, Hochberg Y. Controlling the false discovery rate: a practical and powerful approach to multiple testing. *J Royal Statistical Soc B.* 1995;57:289-300.

Table I. Characteristics of WT and Lepr$^{db/db}$ mice

	BW	sBP	PG	IRI	LP
WT	25.7 ± 0.9	90.3 ± 6.6	120 ± 27	51 ± 30	2457 ± 837
Lepr$^{db/db}$	28.0 ± 1.8†	92.5 ± 12.0	239 ± 21†	278 ± 131†	45726 ± 8585†

Measurements were made on the day of surgery that were fasted for 6h (n=5). Each value is means ± S.E. BW indicates body weight (g); sBP systolic blood pressure (mmHg); PG, plasma glucose (mg/dl); IRI, immunoreactive insulin (μU/ml) and LP, Leptin (pg/ml). † values are significantly different in Lepr$^{db/db}$ mice compared to WT mice ($p<0.05$).

Table II. Pathways Analysis Network for Lepr$^{db/db}$ mice on day 14 post-surgery compared to baseline (p<0.01) superimposed on network for WT mice

Transcript symbol	Transcript name	Fold change
EIF4E	Eukaryotic translation initiation factor 4E	-2.3
ETF1	Eukaryotic translation termination factor 1	-2.3
HSPB8	Heat shock 22kDa protein 8	-3.2
NID	Nidogen	2.8
PABPC1	Poly(A) binding protein, cytoplasmic 1	2.8
PSMA6	Proteasome (prosome, macropain) subunit, alpha type, 6	-2,2
PSMB2	Proteasome (prosome, macropain) subunit, beta type, 2	-2.0
PSMB7	Proteasome (prosome, macropain) subunit, beta type, 7	-2.4
TFPI	Tissue factor pathway inhibitor	2.9
TIMP4	Tissue inhibitor of metalloproteinase 4	-3.1

Table III. Primers for QRT-PCR

Transcript name	5'-Forward primer-3'	5'-Reverse Primer-3'	Accession code	Transcript symbol
Elastin	CTACGGACTGCCCTATACCAATG	GAGTTCCAGCGCCTGCAAT	NM007925	Eln
Glyceraldehyde-3-phosphate dehydrogenase	ACTCCACTCACGGCAAATTCA	GGCCTCACCCCATTTGATG	NM001001303	Gapdh
Neuropilin-1	CCGAGAAAACAAGGTGTTCATG	CGTCCGAAGCTCAGGTGTGT	NM008737	Nrp1
Vascular endothelial growth factor A	CTGTACCTCCACCATGCCAAGT	CTTCGCTGGTAGACATCCATGA	NM009505	Vegfa